Influences of Mold Fungi Colonization on Wheat Straw–Polypropylene Composites

Chunxia He Xuexia Yao Jiao Xue
Jing Xiong Limei Zhao

Abstract

Wheat straw–polypropylene (PP) composites were formed by mixing compression molding to evaluate the susceptibility to mold fungi colonization. The surface morphology, water absorption, Fourier transform infrared spectroscopy (FT-IR), and color variation of the wheat straw–PP composites were investigated before and after colonization with five kinds of mold fungi (after 1, 2, 3, and 4 wk). Macromorphologic and micromorphologic observations indicated fungal colonization was not obvious during the first week, and the wheat straw was perfectly encapsulated in the PP matrix. The original cracks became small holes when the outer wheat straw at the top surface was degraded after fungal colonization for 2 weeks. Consequently, the inner wheat straw was exposed to the fungal environment, and fungal colonization increased. Similar change trends were obtained through FT-IR spectra and color-change analyses. Some characteristic peak ratios in the FT-IR spectra were calculated to investigate the relative degradation rate. Results showed that the fungi used in this study preferentially degraded hemicellulose, followed by lignin, and then cellulose. The carbonyl and lignin indices were used to illustrate the loss in wheat straw mass during the process of colonization. The carbonyl index showed good correlation with the color change. A similar conclusion was obtained for the lignin index. The correlation analyses suggest color change has a close relationship to the process of degradation in wheat straw.

With environmental deterioration and the depletion of natural resources, greater attention is being focused on the study of wood–plastic composites (WPCs). WPCs can be used outdoors, in place of wood and other materials, as planking, guardrails, tables, chairs, and landscape materials. WPCs are generally viewed as inherently more durable structural materials than are untreated woods of the same species because the plastic matrix encapsulates the wood and slows moisture uptake (Wolcott 1996). However, a number of tests have suggested that wood is incompletely encapsulated by the polymer matrix (Kamdem et al. 2004, Yildiz et al. 2005), and the wood component in WPCs may allow moisture levels suitable for fungal attack in outdoor situations. To investigate decay patterns and the effects of fungal degradation on the physical and mechanical properties of WPCs, many studies have tested mass loss, color change, and mechanical differences before and after fungal decay and have used many methods to improve the durability of WPCs against degradation by fungi (Mankowski and Morrell 2000; Schirp and Wolcott 2005; Yildiz et al. 2005; Hosseinaei et al. 2012; Fang et al. 2013; Farahani and Banikarim 2013; Gitchaiwat et al. 2013; Kartal et al. 2013; Kord et al. 2013, 2014; Li et al. 2013; Bazant et al. 2014; Kositchaiyong et al. 2014a, 2014b; Liu et al. 2014; Machovsky et al. 2014; Xu et al. 2014). Morris and Cooper (1998) first showed the presence of fungal decay and discoloration on WPC decking material in service. Mankowski and Morrell (2000) examined the ability of white- and brown-rot fungi to colonize WPCs by measuring mass loss and anatomic changes. WPCs containing a 70:30 wood:high-density polyethylene mixture were found to be the most susceptible to fungal attack. Many types of composites were investigated by Yildiz et al. (2005) with *Coniophora puteana* and *Coriolus versicolor* decay fungi. Their results showed

The authors are, respectively, Professor and PhD Supervisor, Associate Professsor, Master's Candidate, Master's Candidate, and Master's Candidate, College of Engineering, Nanjing Agric. Univ./Key Lab. of Intelligence Agric. Equipment, Nanjing, China (chunxiahe@tom.com [corresponding author], yaoxuexia@njau.edu.cn, 131699406@qq.com, 781842194@qq.com, zhaolimei0610@sina.com). This paper was received for publication in January 2015. Article no. 15-00004.

Forest Prod. J. 66(7/8):472–479.
doi:10.13073/FPJ-D-15-00004

that the quality of the composites decreased, and the extent of decline was related to the polymer type and dosage of wood powder.

However, most studies have investigated WPC resistance to fungal decay based on decay fungi (e.g., brown-rot fungus or white-rot fungus). Relatively few studies (Dawson-Andoh et al. 2004; Hosseinaei et al. 2011, 2012; Liu et al. 2014; Kositchaiyong et al. 2014b; Xu et al. 2015) have used mold fungi to colonize WPCs. Thus, this study was initiated to evaluate the susceptibility of wheat straw–PP composites to mold fungi. Five types of mold fungi (*Aspergillus niger, Chaetomium globosum, Aureobasidium pullulans, Gliocladium virens,* and *Penicillium pinophilum*) were incubated according to the ASTM G21-96 standard (ASTM International 2002). The surface morphology, color change, and water absorption parameters of the wheat straw–PP composite were investigated before and after colonization with five types of mold fungi (at 1, 2, 3, and 4 wk). In addition, the Fourier transform infrared spectroscopy (FT-IR), under various colonization times, was used to analyze the chemical structure of the surface of the wheat straw–PP composites exposed to mold fungi to better understand the degradation mechanisms.

Experimental

Materials

The wheat straw was supplied by Jiangyin Huangtang Co. (China). The wheat straw was crushed to flour, and its particle size was less than 250 μm. The flour was oven-dried at 105°C for 24 hours to remove moisture. The silane coupling agent (KH-550) was obtained from Shanghai Yaohua Co. (China). The PP plastic film (Jiangyin Dongfang Plastic Packaging Co., China) had a melt flow index of 7 to 10 g/10 min and a density of 0.9 g/cm^3.

Methods

Preparation of wheat straw–PP composites.—The amount of KH-550 silane coupling agent was fixed at 2 percent of the wheat straw. KH-550 and ethanol were mixed at the ratio of 1:5. A speed mixer (K600-3205; Braun Electric, Germany) was used to mix wheat straw fiber thoroughly when the KH550 silane solution was sprayed on the wheat straw. The fiber mixture was then dried at 105°C for 12 hours. The pretreated wheat straw was mixed with PP film in an open rubber-mixing machine (X-160 Banbury Mixer; Chuangcheng Rubber and Plastic Machinery Co., Wuxi, China) at a front-roller temperature of 175°C and a back-roller temperature of 170°C for 5 minutes. Then, the mixed compounds were transformed into sheet specimens with a hot-press machine (XLB-0 Vulcanizing Machine; Shunli Rubber Machinery Co., Huzhou, China) with a steel mold (dimensions, 120 by 100 by 5 mm) under a molding temperature of 180°C and a holding pressure of 12.5 MPa for 12 minutes of molding time. The mass ratio of the wheat straw to the PP was controlled at 50:50 for all blends. Finally, the wheat straw–PP composites were cut to 100 by 10 by 5 mm before testing.

Mold resistance test.—According to the ASTM (2002) G21-96 standard, five types of mold fungi (*A. niger, C. globosum, A. pullulans, G. virens,* and *P. pinophilum*) were vaccinated into a potato–glucose medium. The molds were then cultured at a certain temperature and humidity for 7 to 20 days. Five types of spore suspensions were configured to the same concentration with a nutrient solution and were mixed equally and sprayed onto the surface of the wheat straw–PP composites. The composites were then placed into boxes (with constant temperature and humidity) to be colonized at the following experimental conditions: temperature, 28°C; humidity, 85 percent; and time, 1, 2, 3, and 4 weeks.

Micromorphology analysis.—To visualize the extent of colonization, a SMZ1000 stereomicroscope (Nikon Instruments, Minato, Tokyo, Japan) was used to observe the microstructure at the top surface of the wheat straw–PP composites.

Water absorption.—The water absorption of the wheat straw–PP composite was measured according to GB/T 1934.1-2009 standard (Standardization Administration of China 1992). The initial specimens were dried at 60°C for 4 hours. Then, the specimens were immersed in distilled water for 6 hours. The water on the surface of the specimens was dried with filter paper and subsequently weighed. The specimens were again weighed after 1, 2, 4, and 8 days of soaking in distilled water. The maximum water absorption was reached when the difference between the rate of water absorption between the two times was less than 5 percent. The water absorption of the specimens was measured according to the following formula:

$$A = \frac{m_t - m_0}{m_0} \times 100 \quad (1)$$

where A is the water absorption, m_0 is the initial weight after drying, and m_t is the weight after t time of immersion. The result was an average of five specimens.

FT-IR analyses.—FT-IR absorption data were obtained using Nicolet iS-10 (Thermo Fisher Scientific, USA). The 0.002-g specimens, obtained from the top surface of the wheat straw–PP composite, were ground and dispersed in a matrix of potassium bromide, followed by compression to form pellets. FT-IR spectra were recorded in a range from 4,000 to 400 cm^{-1} at a resolution of 4 cm^{-1} using 32 scans. The result was an average of five specimens.

A typical method for analyzing degradation consists of monitoring one or more bands of interest in relation to a band that does not change during the colonization process. Because the peak, at 2,918 cm^{-1}, corresponded to the asymmetric stretching vibrations of methylene (–CH–), the groups that showed the least change during degradation were used as a reference (Zhang et al. 1997, 2008). The peak at 1,739 cm^{-1} is often attributed to the contribution of hemicelluloses because it is a result of the stretching of carbonyl groups (C=O) in the hemicelluloses. The carbonyl index, defined in a previous study (Stark and Matuana 2004), was calculated as follows:

$$\text{Carbonyl index} = \frac{I_{1,739}}{I_{2,913}} \quad (2)$$

where I denotes the intensity. The peak intensity in the carbonyl region was normalized to the intensity of the peak at 2,918 cm^{-1}, which corresponds to the asymmetric stretching vibrations of the methylene groups. The peak value at 1,508 cm^{-1} is often attributed to the contribution of lignin because it arises purely from aromatic skeletal

vibrations (C=C) in lignin. Thus, the lignin index was calculated as follows:

$$\text{Lignin index} = \frac{I_{1,508}}{I_{2,918}} \quad (3)$$

where I denotes the intensity. The peak intensity of aromatic skeletal vibration originating from lignin (1,508 cm^{-1}) was also normalized using the intensity of the peak at 2,918 cm^{-1}.

Color measurement.—The surface color, before and after mold colonization of the composites, was measured with a chroma meter (HP200; Hanpu, China) according to the Commission Internationale de l'Echlairage (1976) CIELAB 1976 $L^*a^*b^*$ color system, where L^* represents the lightness coordinate and varies from 100 (white) to 0 (gray); a^* (with values from +150 to −150) represents the red ($+a^*$) to green ($-a^*$) coordinates; and b^* (with values from +150 to −150) represents the yellow ($+b^*$) to blue ($-b^*$) coordinates. The color change was calculated according to Equation 4:

$$\Delta E^* = \left[(\Delta L^*)^2 + (\Delta a^*)^2 + (\Delta b^*)^2\right]^{1/2} \quad (4)$$

where ΔL^*, Δa^*, and Δb^* represent the difference between before and after colonization. The surface color was measured at six locations on each specimen.

Results and Discussion

The surface macroscopic morphology of the wheat straw–PP composite

Following the ASTM G21 standard, the scale for observing the visual effects of fungal growth at the top surfaces of WPCs with different colonization times is listed in Table 1. The surface degradation of the composite became more serious with increased exposure time to the mold fungi. In the early stage of a fungal attack, the fungal colonization was not obvious, and the extent of degradation was only rated at Level 1 after 1 week of colonization. The degradation intensified, however, after 2 weeks of colonization, and the mold coverage quickly reached Level 3. The fungal growth reached Level 4 quickly after 3 weeks of colonization.

The detailed macroscopic surface topography is shown in Figure 1. Some small, white mold was observed at the cut section of the specimens after 1 week of colonization. Many hyphae were visible at the cut side, and a few hyphae could also be observed on the top surface after 2 weeks of colonization. The hyphae grew further, and the top surface of the specimens had many white hyphae after 4 weeks of colonization.

According to observations of the macroscopic morphology, the fungal growth started from the cut surfaces of the specimens, and because of that, the biodegradation of the PP was very limited. The wheat straw at the cut side, which was not wrapped in the PP matrix, was accessible to fungal attack. Microscopic morphology was used to further analyze the details of the degradation process.

The surface microscopic morphology of the wheat straw–PP composite

Figure 2 shows the surface microcosmic topography of the wheat straw–PP composites under different periods of colonization. As shown, before colonization, the top surface of the specimens was relatively smooth, with only some small cracks in local regions, and the wheat straw was mainly encapsulated by the PP matrix. After 1 week of fungal attack, the exposed wheat straw at the top surface served not only as points of moisture uptake but also as a source of nutrients for the fungal propagules that settled on the top surfaces. Fungal colonization was initiated and anchored at those sites. The original cracks became small holes after 2 weeks of fungal attack. The extent of the degradation was more severe and the holes became bigger after 3 weeks of exposure to the mold fungi. The holes became larger and deeper after 4 weeks of colonization.

Table 1.—The growth levels of the mold within the composites after different colonization times.[a]

Colonization time (wk)	Coverage levels
0	0
1	1
2	3
3	4
4	4

[a] 0 = no decay; 1, 2, 3, and 4 = microbial growth at <10 percent, 10 to 30 percent, 30 to 60 percent, and >60 percent coverage, respectively.

Macromorphologic and micromorphologic observations demonstrated that mold fungi first colonized the wheat straw on the cut side; then, the exposed wheat straw on the top surface was attacked, and the inner wheat straw was the last to be degraded. Because the wheat straw on the top surface was nearly encapsulated by the PP matrix, the colonization was inconspicuous during the first week. The original cracks became small holes when the wheat straw on the top surface was degraded. Finally, the inner wheat straw was exposed to the fungal environment, and degradation increased after 2 weeks of colonization.

Wheat straw–PP composite water absorption after different colonization times

Water absorption is a good performance indicator of susceptibility to fungal attack for materials that use nondurable wheat straw without supplemental fungicidal protection. Water absorption achieved by the wheat straw–PP composites after different colonization times is shown in Figure 3. The data in Figure 3 indicate that the water absorption was lowest for the wheat straw–PP composite before colonization, and the corresponding value was only 13.15 percent when soaked in distilled water for 192 hours. However, water absorption by the wheat straw–PP composite after 1 week of colonization had risen to 18.42 percent. Water absorption after colonization for 2, 3, and 4 weeks was similar, with values of 20.43, 20.66, and 20.68 percent, respectively.

According to the trend of the changes in water absorption, we speculated that the inner wheat straw was mainly encapsulated by the hydrophobic PP matrix after 1 week of colonization, so the water absorption of the composites was less than it was during subsequent weeks. The exposed wheat straw at the top surface, however, was degraded after 2 weeks of colonization; the initial cracks became small holes, and the inner, hydrophilic wheat straw was largely exposed to the mold fungal environment. This resulted in

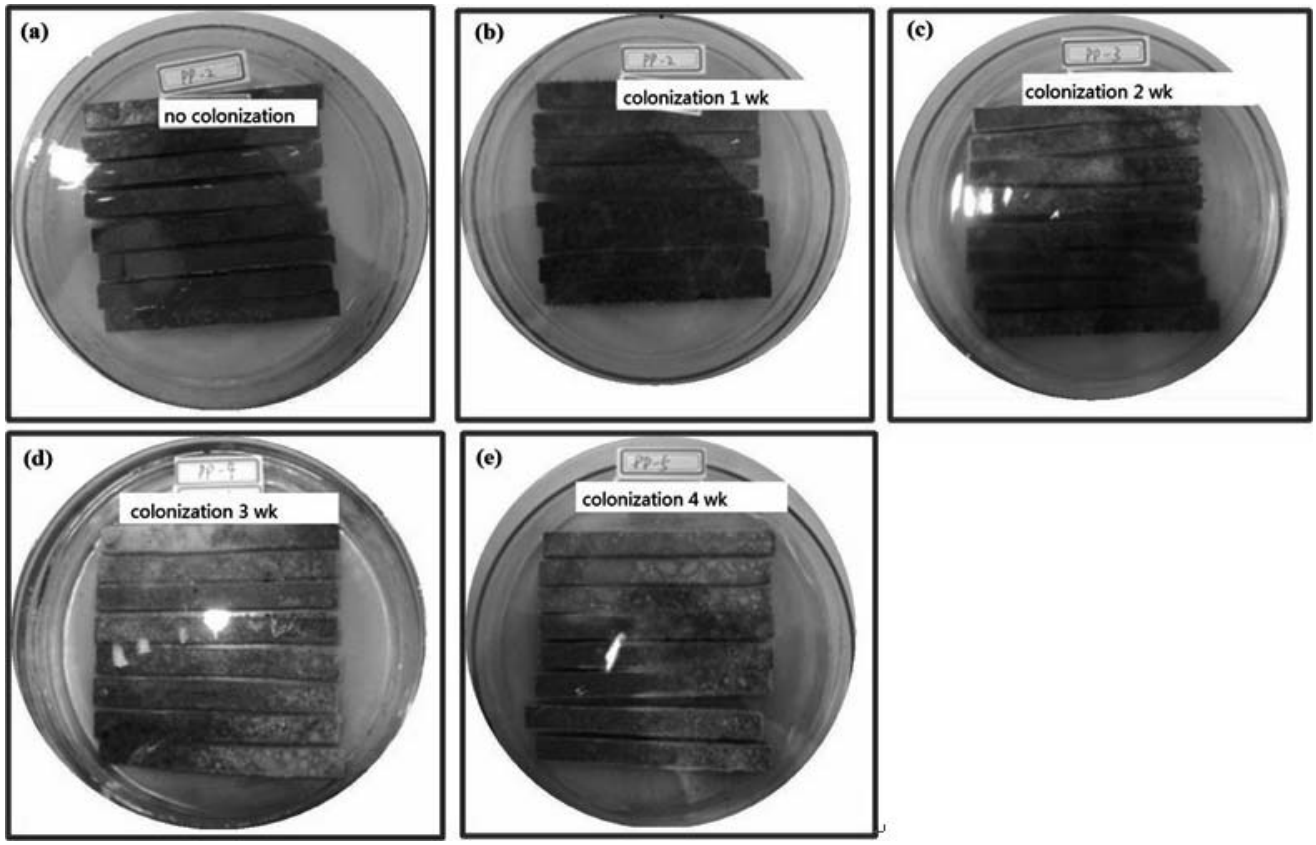

Figure 1.—Macrostructure surface of wheat straw–polypropylene composites with different colonization times: (a) no colonization, (b) colonization for 1 week, (c) colonization for 2 weeks, (d) colonization for 3 weeks, and (e) colonization for 4 weeks.

similar water absorption rates for the composites during the remaining colonization periods.

FT-IR spectra of wheat straw–PP composites at different colonization times

In this study, the FT-IR spectra were used to analyze surface chemical changes of the wheat straw–PP composites caused by the effects of fungal attack. The FT-IR spectra of the wheat straw–PP composites under various colonization times are shown in Figure 4. The values of main characteristic peaks for the wheat straw–PP composites are also displayed in Figure 4. The main characteristic bands of the FT-IR spectra of the wheat straw–PP composites are presented in Table 2.

As shown in Figure 4, most absorption peaks reduced gradually with an increase in colonization time. The biodegradability of the PP matrix was limited. Thus, a calculation of the mass loss was based on the wheat straw because it represents the main fungal food source within the composite. Because the mass loss was not measured in this study, the carbonyl index and lignin index were used to analyze the mass loss during the process of colonization. The changes for the carbonyl and lignin indices at various colonization times are plotted in Figures 5 and 6, respectively. As shown in Figures 5 and 6, the carbonyl index and the lignin index decreased slowly during the first week but decreased faster during the remaining 3 weeks. The trend of the change for the carbonyl and lignin indices

Table 2.—Characteristic bands of the infrared spectra for the wheat straw–polypropylene composites.

Wave numbers (cm^{-1})	Functional group	Assignment
3,423	O–H	O–H stretch (hydrogen bond)
1,739	−COOH(C=O)	Free carbonyl groups, stretching of acetyl or carboxylic acid (hemicelluloses)
1,635	C=O	C=O stretching vibration in conjugated carbonyl of lignin
1,508	C=C	C=C stretching of the aromatic ring (lignin)
1,457	C–H	Asymmetric bending in CH_3 (lignin)
1,376	C–H	C–H deformation in cellulose and hemicellulose
1,255	C–O	Guaiacyl ring breathing with CO-stretching (lignin and hemicelluloses), esters
1,165	C–O–C	Carbohydrate (in cellulose)
1,053	C–O	C–O stretch in cellulose and hemicellulose
898	C–H	C–H deformation in cellulose
2,952, 2,918, and 2,838	C–H	C–H stretching of PP

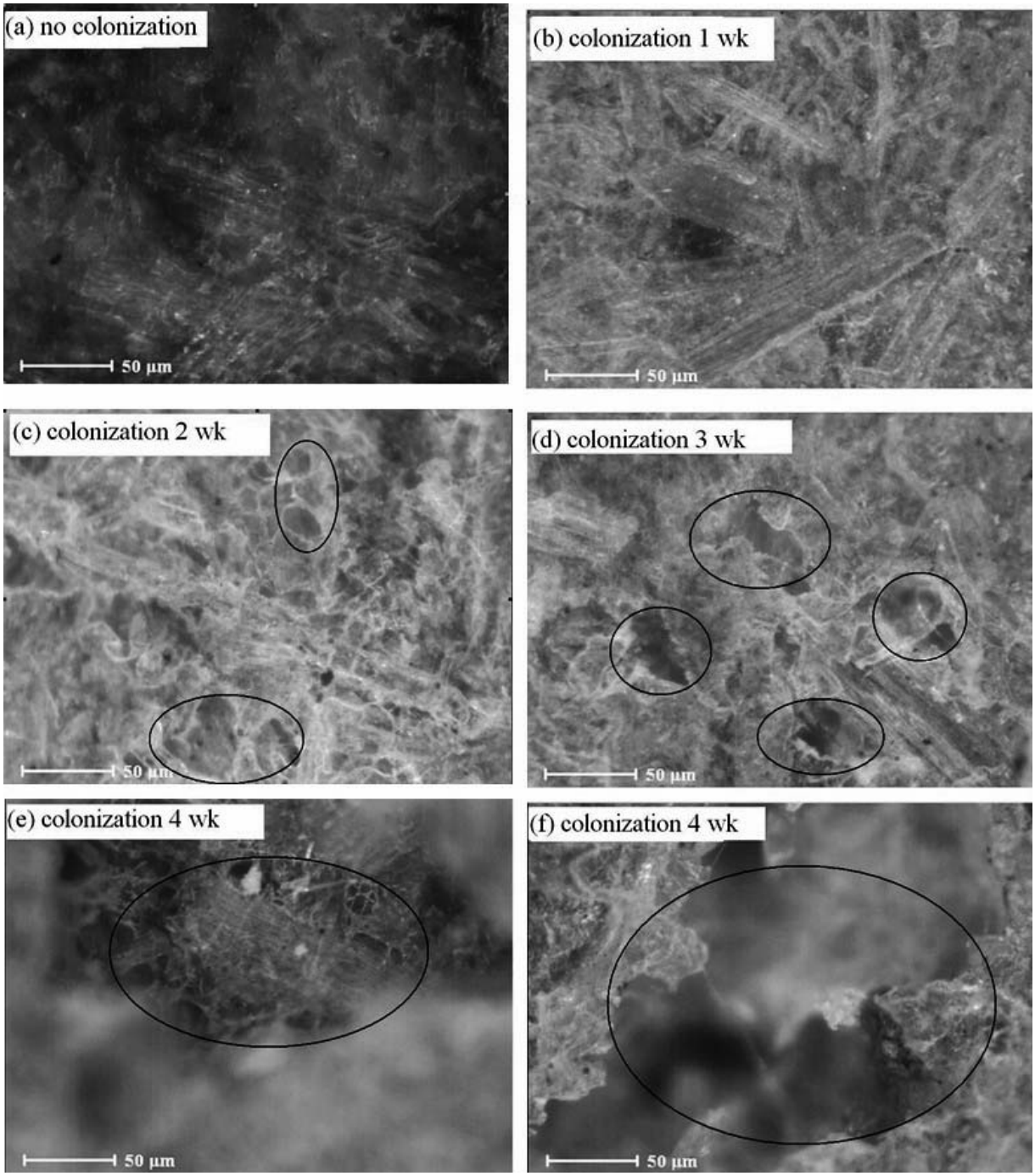

Figure 2.—Microstructure surface of wheat straw–polypropylene composites with different periods of decay: (a) no colonization, (b) colonization for 1 week, (c) colonization for 2 weeks, (d) colonization for 3 weeks, (e) colonization for 4 weeks, and (f) colonization for 4 weeks. (The degraded holes are denoted with circles.)

was consistent with our macromorphologic and micromorphologic observations.

Wheat straw is mainly composed of cellulose, hemicellulose, and lignin. The mass change of these three components can provide important information toward understanding the detailed process of colonization by mold fungi. The peak value, at 1,739 cm^{-1}, was caused by C=O stretching in the hemicellulose (see Table 2). The peak value at 1,508 cm^{-1} arose purely because of the aromatic skeletal vibration (C=C) in the lignin. The peak value of 1,255 cm^{-1} was caused by the stretching in the phenol–ether bonds of the lignin, whereas the 1,376, 1,165, and 898 cm^{-1} peaks were because of the structural contributions of cellulose and hemicellulose. Similar to a previous study (Xu et al. 2013), we calculated several peak ratios (listed in Table 3) to investigate the relative degradation rate of cellulose, hemicellulose, and lignin during the process of colonization. The value of $I_{1,739}$/

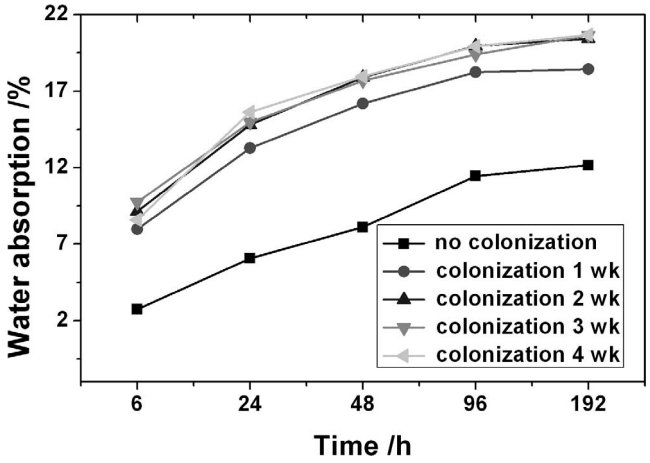

Figure 3.—Water absorption of wheat straw–polypropylene composites with different colonization times.

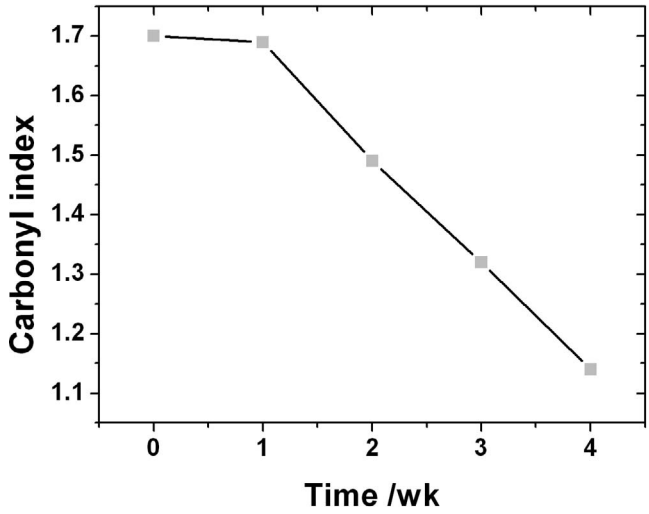

Figure 5.—Carbonyl index of wheat straw–polypropylene composites with different colonization times.

$I_{1,508}$ decreased from 1.18 to 1.05 after 4 weeks of colonization, which showed that the degradation rate of hemicellulose was greater than that of lignin. In addition, $I_{1,255}/I_{1,739}$ ratios increased from 0.81 to 0.95 after the 4-week colonization, which proved that the fungi had a relatively weaker capacity for degrading lignin compared with degrading hemicellulose. The values of $I_{1,376}/I_{1,508}$, $I_{1,165}/I_{1,508}$, and $I_{898}/I_{1,508}$ increased from 0.71 to 0.94, from 0.69 to 0.95, and from 1.06 to 1.21, respectively, after 4 weeks of colonization. These increases could be attributed to the lessened ability of the fungi to degrade the cellulose compared with the lignin. These data suggest that the fungi used in this study preferentially degraded hemicellulose, followed by lignin, and then cellulose.

Color change in the wheat straw–PP composite at different colonization times

The color differences before and after fungal degradation of wheat straw–PP composites are listed in Table 4 at various colonization times. The value of the color change was bigger when the material degradation was more obvious. The data in Table 4 indicate that the mold fungal degradation caused greater color change (ΔE^*) in the composites with an increase in the time of colonization. The data in Table 4 also show that the ΔL^* and Δa^* were both positive. It indicates that the color changes in the wheat straw–PP composites were in the direction of white and red with prolonged colonized time. Therefore, the mold fungal degradation resulted in a discoloration of the composites. The value of the composites' Δb^* became negative during the initial 3-week colonization. This shows that wheat straw–PP composite changes were in the direction of blue. The value of the composites' Δb^* became positive after 4 weeks of colonization, which suggests that, after 4 weeks of colonization, the wheat straw–PP composite degradation was in the yellow direction.

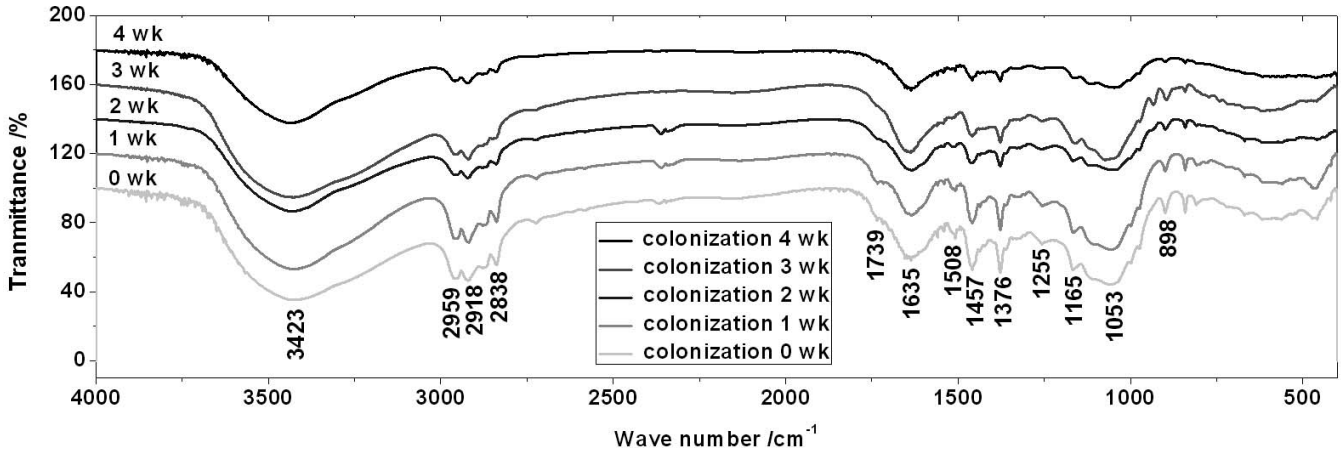

Figure 4.—Fourier transform infrared spectroscopy spectra from wheat straw–polypropylene composites with different colonization times.

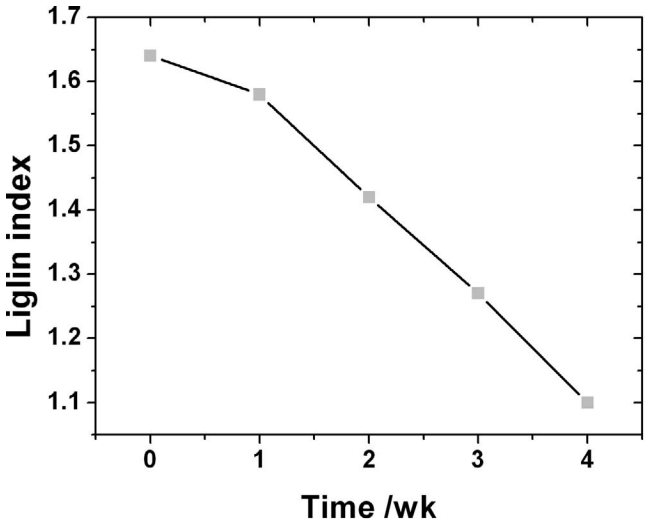

Figure 6.—Lignin index of wheat straw–polypropylene composites with different colonization times.

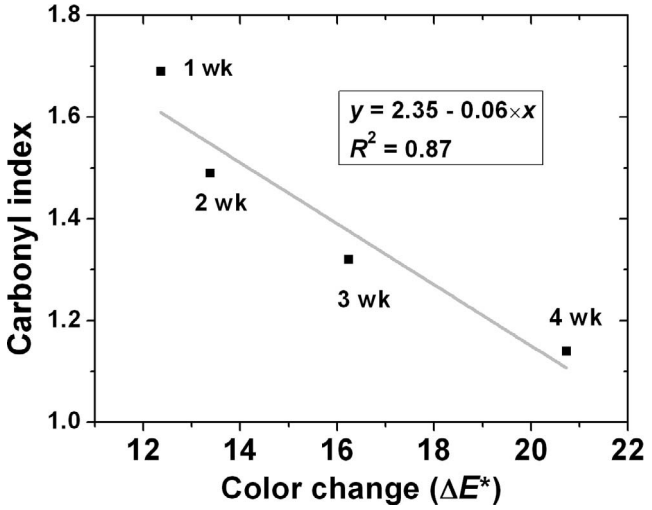

Figure 7.—The correlation between the carbonyl index and the change in color (ΔE) for the wheat straw–polypropylene composites.*

Table 3.—Relative intensities of characteristic peaks for carbohydrates and lignin for the wheat straw at different colonization times.

Colonization time (wk)	$I_{1,739}/I_{1,508}$	$I_{1,376}/I_{1,508}$	$I_{1,165}/I_{1,508}$	$I_{898}/I_{1,508}$	$I_{1,255}/I_{1,739}$
0	1.18	0.71	0.69	1.06	0.81
1	1.09	0.72	0.74	1.11	0.83
2	1.07	0.82	0.82	1.13	0.89
3	1.06	0.87	0.90	1.14	0.92
4	1.05	0.94	0.95	1.21	0.95

Table 4.—The color change before and after fungal degradation of wheat straw–polypropylene composites under different colonization times.

Colonization time (wk)	ΔL^*	Δa^*	Δb^*	ΔE^*
1	12.36	2.63	−0.8	12.66
2	13.38	2.35	−2.34	13.78
3	16.24	1.79	−1.43	16.41
4	20.73	3.38	1.93	20.09

The degradation of the composites resulted in both mass loss and color change. Therefore, the mass loss most likely had some correlation with the color change. Because direct weight loss was not measured, the correlation map between the carbonyl index and the color change was plotted (shown in Fig. 7). The data in Figure 7 show that the carbonyl index correlated well with the change in color, and the corresponding determination coefficient was up to 0.87. The lignin index had relatively better correlation with the color change, and the determination coefficient reached 0.90 (see Fig. 8). The correlation analyses suggest that the color change had a close relationship with the degradation of the wheat straw. Dawson-Andoh et al. (2004) also proved that fungal colonization resulted in discoloration of rigid polyvinyl chloride–wood-flour composites.

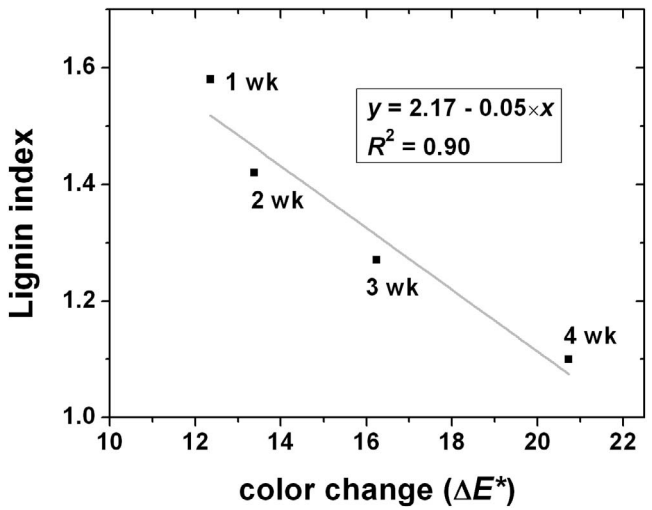

Figure 8.—The correlation between the lignin index and the change in color (ΔE) of the wheat straw–polypropylene composites.*

Conclusions

Macromorphologic and micromorphologic observations showed that degradation was not obvious during the first week of fungal attack, and the wheat straw was nearly encapsulated by the PP matrix. The original cracks became small holes when the top surface of the wheat straw was degraded after 2 weeks of colonization. Afterward, the inner wheat straw was exposed to the fungal environment, and the fungal degradation increased. Similar change trends were observed in the FT-IR spectra and with the color-change analysis. The ratios of several characteristic peaks in the FT-IR spectra were calculated to investigate the relative degradation rate of cellulose, hemicellulose, and lignin. The results suggested that the mold fungi used in this study preferentially degraded hemicellulose, followed by lignin, then cellulose.

The carbonyl and lignin indices were used to illustrate the mass loss in the wheat straw during the process of colonization. The carbonyl index had particularly good correlation with color change, and similar results were obtained with the lignin index. The correlation analysis suggests that color change has a close relationship with the degradation of wheat straw.

Acknowledgments

This work was supported by the National Natural Science Foundation of China (Grant No. 41301261), Natural Science Foundation of Jiangsu Province (Grant No. BK20130680), and Postdoctoral Science Foundation of China (Grant No. 2015M571765).

Literature Cited

ASTM International. 2002. Standard practice for determining resistance of synthetic polymeric materials to fungi. ASTM G21-96. ASTM, West Conshohocken, Pennsylvania.

Bazant, P., I. Kuritka, O. Hudecek, M. Machovsky, M. Mrlik, and T. Sedlacek. 2014. Microwave-assisted synthesis of Ag/ZnO hybrid filler, preparation, and characterization of antibacterial poly(vinyl chloride) composites made from the same. *Polym. Compos*. 35:19–26.

Commission Internationale de l'Echlairage. 1976. ISO 11664-4:2008(E)/ CIE S 014-4/E:2007 joint ISO/CIE standard: Colorimetry, part 4—CIE 1976 L*a*b* colour space. CIE Central Bureau, Vienna.

Dawson-Andoh, B., L. M. Matuana, and J. Harrison. 2004. Mold susceptibility of rigid PVC/wood-flour composites. *J. Vinyl Addit. Technol*. 10:179–186.

Fang, Y. Q., Q. W. Wang, C. G. Guo, Y. M. Song, and P. A. Cooper. 2013. Effect of zinc borate and wood flour on thermal degradation and fire retardancy of polyvinyl chloride (PVC) composites. *J. Anal. Appl. Pyrolysis* 100:230–236.

Farahani, M. R. M. and F. Banikarim. 2013. Effect of nano-zinc oxide on decay resistance of wood–plastic composites. *BioResources* 8:5715–5720.

Gitchaiwat, A., A. Kositchaiyong, K. Sombatsompop, B. Prapagdee, K. Isarangkura, and N. Sombatsompop. 2013. Assessment and characterization of antifungal and antialgal performances for biocide-enhanced linear low-density polyethylene. *J. Appl. Polym. Sci*. 128:371–379.

Hosseinaei, O., S. Q. Wang, T. G. Rials, C. Xing, A. M. Taylor, and S. S. Kelley. 2011. Effect of hemicellulose extraction on physical and mechanical properties and mold susceptibility of flakeboard. *Forest Prod. J*. 61:31–37.

Hosseinaei, O., S. Q. Wang, A. M. Taylor, and J. W. Kim. 2012. Effect of hemicellulose extraction on water absorption and mold susceptibility of wood–plastic composites. *Int. Biodeterior. Biodegrad*. 71:29–35.

Kamdem, D. P., H. H. Jiang, W. N. Cui, J. Freed, and L. M. Matuana. 2004. Properties of wood plastic composites made of recycled HDPE and wood flour from CCA-treated wood removed from service. *Compos. Part A Appl. Sci. Manuf*. 35:347–355.

Kartal, S. N., S. Aysal, E. Terzi, N. Yilgor, T. Yoshimura, and K. Tsunoda. 2013. Wood and bamboo–PP composites: Fungal and termite resistance, water absorption, and FT-IR analyses. *BioResources* 8:1222–1244.

Kord, B., S. K. Hosseinihashemi, and M. Modirzare. 2013. Influence of fungal infection on the long-term water absorption and morphological behavior of bagasse fiber/polypropylene composites at different exposure times. *Sci. Eng. Compos. Mater*. 20:351–357.

Kord, B., E. Jari, A. Najafi, and V. Tazakorrezaie. 2014. Effect of nanoclay on the decay resistance and physicomechanical properties of natural fiber-reinforced plastic composites against white-rot fungi (*Trametes versicolor*). *J. Thermoplast. Compos. Mater*. 27:1085–1096.

Kositchaiyong, A., V. Rosarpitak, H. Hamada, and N. Sombatsompop. 2014a. Anti-fungal performance and mechanical morphological properties of PVC and wood/PVC composites under UV-weathering aging and soil-burial exposure. *Int. Biodeterior. Biodegrad*. 91:128–137.

Kositchaiyong, A., V. Rosarpitak, and N. Sombatsompop. 2014b. Antifungal properties and material characteristics of PVC and wood/ PVC composites doped with carbamate-based fungicides. *Polym. Eng. Sci*. 54:1248–1259.

Li, Y. F., Z. B. Liu, X. Y. Dong, Y. L. Fu, and Y. X. Liu. 2013. Comparison of decay resistance of wood and wood-polymer composite prepared by in-situ polymerization of monomers. *Int. Biodeterior. Biodegrad*. 84:401–406.

Liu, R., Y. Peng, J. Z. Cao and S. P. Luo. 2014. Water absorption, dimensional stability, and mold susceptibility of organically modified–montmorillonite modified wood flour/polypropylene composites. *BioResources* 9:54–65.

Machovsky, M., I. Kuritka, P. Bazant, D. Vesela, and P. Saha. 2014. Antibacterial performance of ZnO-based fillers with mesoscale structured morphology in model medical PVC composites. *Mater. Sci. Eng. C Mater. Biol. Appl*. 41:70–77.

Mankowski, M. and J. J. Morrell. 2000. Patterns of fungal attack in wood-plastic composites following exposure in a soil block test. *Wood Fiber Sci*. 32:340–345.

Morris, P. I. and P. Cooper. 1998. Recycled plastic/wood composite lumber attacked by fungi. *Forest Prod. J*. 48:86–88.

Schirp, A. and M. P. Wolcott. 2005. Influence of fungal decay and moisture absorption on mechanical properties of extruded wood-plastic composites. *Wood Fiber Sci*. 37:643–652.

Standardization Administration of China. 1992. Method for determination of the moisture content of wood. GB/T 1934-2009. SAI Global, Paramus, New Jersey.

Stark, N. M. and L. M. Matuana. 2004. Surface chemistry changes of weathered HDPE/wood-flour composites studied by XPS and FTIR spectroscopy. *Polym. Degrad. Stabil*. 86:1–9.

Wolcott, M. P. 1996. The role of thermoplastics in conventional wood composites. *In:* Proceedings of the 30th Washington State University International Particleboard/Composite Materials Symposium, April 16–18, 1996, Washington State University, Pullman. pp. 37–44.

Xu, G. Q., L. H. Wang, J. L. Liu, and J. Z. Wu. 2013. FTIR and XPS analysis of the changes in bamboo chemical structure decayed by white-rot and brown-rot fungi. *Appl. Surf. Sci*. 280:799–805.

Xu, K. M., J. Feng, T. H. Zhong, Z. F. Zheng, and T. A. Chen. 2015. Effects of volatile chemical components of wood species on mould growth susceptibility and termite attack resistance of wood plastic composites. *Int. Biodeterior. Biodegrad*. 100:106–115.

Xu, K. M., K. F. Li, T. H. Zhong and C. P. Xie. 2014. Interface self-reinforcing ability and antibacterial effect of natural chitosan modified polyvinyl chloride-based wood flour composites. *J. Appl. Polym. Sci*. 131:1082–1090.

Yildiz, U. C., S. Yidiz, and E. D. Gezer. 2005. Mechanical properties and decay resistance of wood-polymer composites prepared from fast growing species in Turkey. *Bioresour. Technol*. 96:1003–1011.

Zhang, D., Y. R. Shen, and G. A. Somorjai. 1997. Studies of surface structures and compositions of polyethylene and polypropylene by IR plus visible sum frequency vibrational spectroscopy. *Chem. Phys. Lett*. 281:394–400.

Zhang, Y. X., H. Dou, B. Chang, Z. C. Wei, W. X. Qiu, S. Z. Liu, W. X. Liu, and S. Tao. 2008. Emission of polycyclic aromatic hydrocarbons from indoor straw burning and emission inventory updating in China. *In:* Environmental Challenges in the Pacific Basin. D. O. Carpenter (Ed.). Wiley-Blackwell, Malden, Massachusetts. pp. 218–227.